SCIENTIFIC REPORTS

OPEN

SUBJECT AREAS:
BIOMATERIALS
ATOMIC FORCE MICROSCOPY
BIOLOGICAL PHYSICS
NANOSCALE MATERIALS

Received
1 March 2013

Accepted
23 July 2013

Published
22 August 2013

Correspondence and requests for materials should be addressed to C.T. (teichert@unileoben.ac.at)

What holds paper together: Nanometre scale exploration of bonding between paper fibres

Franz J. Schmied[1,4], Christian Teichert[1,4], Lisbeth Kappel[2,4], Ulrich Hirn[2,4], Wolfgang Bauer[2,4] & Robert Schennach[3,4]

[1]Institute of Physics, Montanuniversität Leoben, 8700 Leoben, Austria, [2]Institute for Paper, Pulp and Fiber Technology, Graz University of Technology, 8010 Graz, Austria, [3]Institute of Solid State Physics, Graz University of Technology, 8010 Graz, Austria, [4]CD-Laboratory for Surface Chemical and Physical Fundamentals of Paper Strength, Graz University of Technology, 8010 Graz, Austria.

Paper, a man-made material that has been used for hundreds of years, is a network of natural cellulosic fibres. To a large extent, it is the strength of bonding between these individual fibres that controls the strength of paper. Using atomic force microscopy, we explore here the mechanical properties of individual fibre-fibre bonds on the nanometre scale. A single fibre-fibre bond is loaded with a calibrated cantilever statically and dynamically until the bond breaks. Besides the calculation of the total energy input, time dependent processes such as creep and relaxation are studied. Through the nanometre scale investigation of the formerly bonded area, we show that fibrils or fibril bundles play a crucial role in fibre-fibre bonding because they act as bridging elements. With this knowledge, new fabrication routes can be deduced to increase the strength of an ancient product that is in fact an overlooked high-tech material.

Paper is a versatile material that has been used for centuries, mainly for exchange of information or for protection and storage of goods. Although its importance for information exchange might decrease with the advent of e-books, its role as a natural and degradable packaging material will by contrast increase. In addition, a variety of quite novel paper based technologies arise at the horizon[1]. These include the application of paper as a novel material platform, e.g. for low-cost (flexible) electronic and energy devices[2,3], for actuators[4] as well as for sensors in medical[5] or environmental[6] diagnostics. The last combines paper with the novel true two-dimensional material graphene. There exist also nanocomposite concepts to complement paper e.g. with magnetic properties[7] or hydrophobicity[8,9]. Despite these unconventional new developments on functionalizing paper for high-technology applications, we focus here on the understanding of the fundamentals of paper strength[10] as a key function for packaging materials. For this purpose and since paper is a composite of natural cellulosic fibres that are bonded to each other by intermolecular forces, measurement of the mechanical properties of individual fibre-fibre bonds provides significant insight into the key processes governing paper's mechanical behaviour.

A single pulp fibre is a wood cell in which the lumen is collapsed and the cell walls stay intact (see the scheme of atomic force microscopy (AFM) images in Figure 1a and the cross-sectional image in Figure 1b). These cell walls consist of cellulose chains which are embedded in a matrix of hemicellulose and lignin[11]. During the drying process in paper fabrication, single pulp fibres approach each other closely enough to form bonds. Figure 1b shows a topography image of a cross-sectional sample prepared by an ultra-microtome cut through a single 90° fibre-fibre bond of unrefined pulp. Several mechanisms have been suggested to play a significant role in forming the fibre-fibre bonds that lead to the fibre network that we call paper. In the past, the following possible bonding mechanisms were considered[12]: hydrogen bonds, mechanical interlocking, electrostatic interactions, interdiffusion of cellulose molecules, and van der Waals forces. More recently, microcompressions[13], capillary bridges[14], and stress due to the drying process[10] have been under discussion. What is agreed is that all of these mechanisms contribute in some way to bonding two pulp fibres together. It is still not clear, however, which of these mechanisms dominates or if an interplay of several mechanisms is relevant. To tackle this question, a method is required to measure the joint strength of a single fibre-fibre bond in a well-defined experiment. The experimental method must meet two requirements. First, it must be able to measure the range of the depicted force with sufficient precision. In macroscopic measurements such as tensile testers[15–22] the range of the depicted force is on the lower bound of instrumental resolution. In nanoscale investigation using novel scanning probe techniques, as

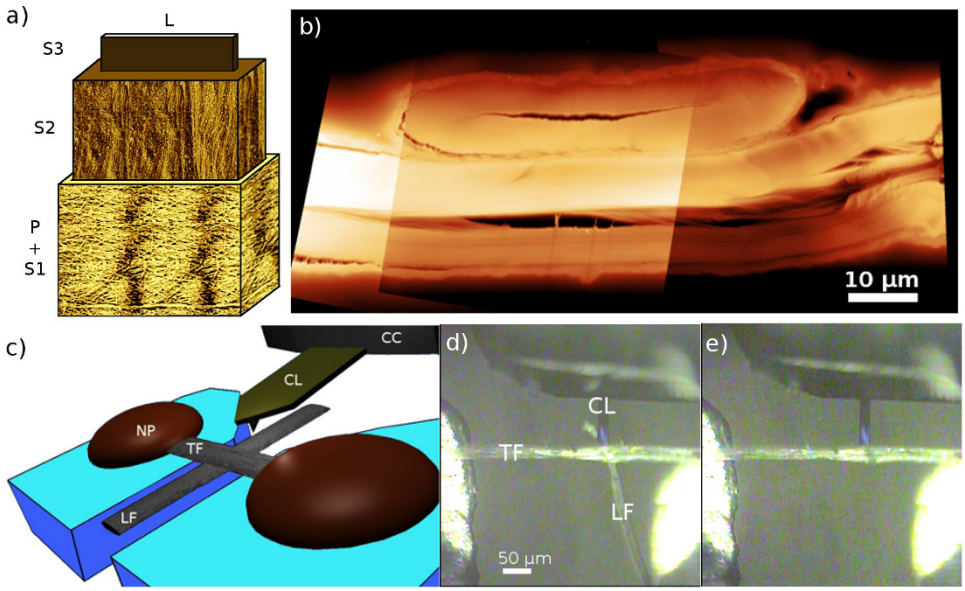

Figure 1 | Introduction to pulp fibres and the experimental approach. (a) AFM phase images of various cell wall layers of a pulp fibre. P-Primary wall, S1-Secondary Wall 1, S2-Secondary Wall 2, S3-Secondary wall 3, and L-Lumen. (b) Stitched AFM topography image of a fibre-fibre bond cross-section embedded in resin. (c) Scheme of the measurement setup in an AFM, Photograph of the setup before (d) and after (e) fibre-fibre bond failure. NP - Nail polish, TF - Top fibre, LF - Lower fibre, CL - Cantilever, CC - Cantilever Chip.

has been performed for carbon nanotubes[23–25], nano wires[26], collagen fibrils[27], and single cellulose fibrils[28], the required force is too high. The same problem occurs when employing microelectromechancial systems (MEMS) technique[29,30]. An average value for fiber-fiber bond strength uses the Page equation based on macroscopical tests on sheets[31].

The second requirement concerns the mode of the applied force[32,33]. To date, joint strength measurements on pulp fibre-fibre bonds have dealt only with shear stresses. In that case, both fibres are straightened and twisted and, thus, it is assumed that in addition to shearing peeling is present. To study the influence of different bonding mechanisms, a new technique has to be developed that works in only one opening mode. The easiest mode is an opening of the fibre-fibre bond in z-direction, where the separation force is lower than for shear bond strength[17].

In addition to bonding mechanisms, time-dependences of paper with respect to load, moisture content, and temperature[34,35] are very important. Indeed, there is an ongoing debate as to whether creep or relaxation occurs within the interfibre bond or depends on structural changes in the fibres themselves[13].

Here, we utilize the nanometre scale probing capabilities of the well established AFM technique[36] to measure the bonding force between two single pulp fibres. A very stiff AFM cantilever is used to apply a defined force into the fibre-fibre bond[37]. The corresponding setup together with AFM results of fibre surfaces and fibre-fibre cross-sections is demonstrated in Figure 1. Figure 1a presents AFM phase images of the secondary wall 1 with remainders of the primary wall (P + S1) and the secondary wall 2 (S2) of a single pulp fibre. A high-resolution AFM topography cross-section of a single fibre-fibre bond embedded in resin is shown in Figure 1b. A scheme of the measurement setup is shown in Figure 1c and photographs of the setup with the fibre-fibre bond before and after failure are presented in Figure 1d,e. After failure of the bond, a dark shadow is visible marking the formerly bonded area (Figure 1e). In addition to analysing the bonding force as a single quantity, the behaviour prior to the failure is analysed. Force discontinuities are correlated with features revealed on the formerly bonded area which is recorded by conventional AFM scanning. This investigation provides new insights into the mechanisms of fibre bonding and their contribution to the fibre-fibre bond. Furthermore, through the fine resolved displacement changes it is possible to access time-dependent behaviours such as creep and relaxation and determine their contribution to total energy input.

Results

Our method allows testing of the bonds via two different approaches[37]. First, we use dynamic loading to determine elastic energy contributions from force-versus-distance curves in a force regime lower than the joint strength. The hysteresis in the individual cycles is a measure of the dissipated energy. Second, a static loading experiment provides further insight into the dissipated energy. Here, the load is kept constant and the movement of the cantilever by the AFM's z-piezo actuator - necessary to maintain constant cantilever bending - is recorded. In this way, we are able to record creeping of the fibre-fibre bond sample, a property inherent to viscoelastic material as has been established, for example, in polymers[33]. Our analysis of the steady-state creep rate reveals an increase with higher load, as has also been reported for aluminium[38].

Figure 2 summarizes the findings of the fibre-fibre bond investigation of unrefined pulp. A stitched AFM topography image of the formerly bonded area is presented in Figure 2a. The image clearly distinguishes between a wrinkled surface in the unbonded region and a smoother surface of the formerly bonded area[39]. At the transition region between bonded and unbonded area, more dangling microfibrils or fibril bundles are visible than on the remaining fibre. These are clear indications of mechanical interlocking or bridging of single fibrils or fibril bundles, similar to assembling of the fibrils itself as introduced first by Keckes et al[40–42]. A comparison of the true surface area (2028 μm^2 as can easily be determined by analysis of the AFM image) and the projected area (1914 μm^2) in Figure 2a revealed that the true surface area of the bonded area is 6–8% larger, mainly enhanced by the dangling fibrils but also due to the fibrillar structure. In contrast to the bonded area, the unbonded region of the fiber surface is enhanced by 20% in terms of true surface area. Furthermore, the resulting lower surface roughness of the bonded area also directly enhances the contribution of the capillary bridges, as we have recently demonstrated[43].

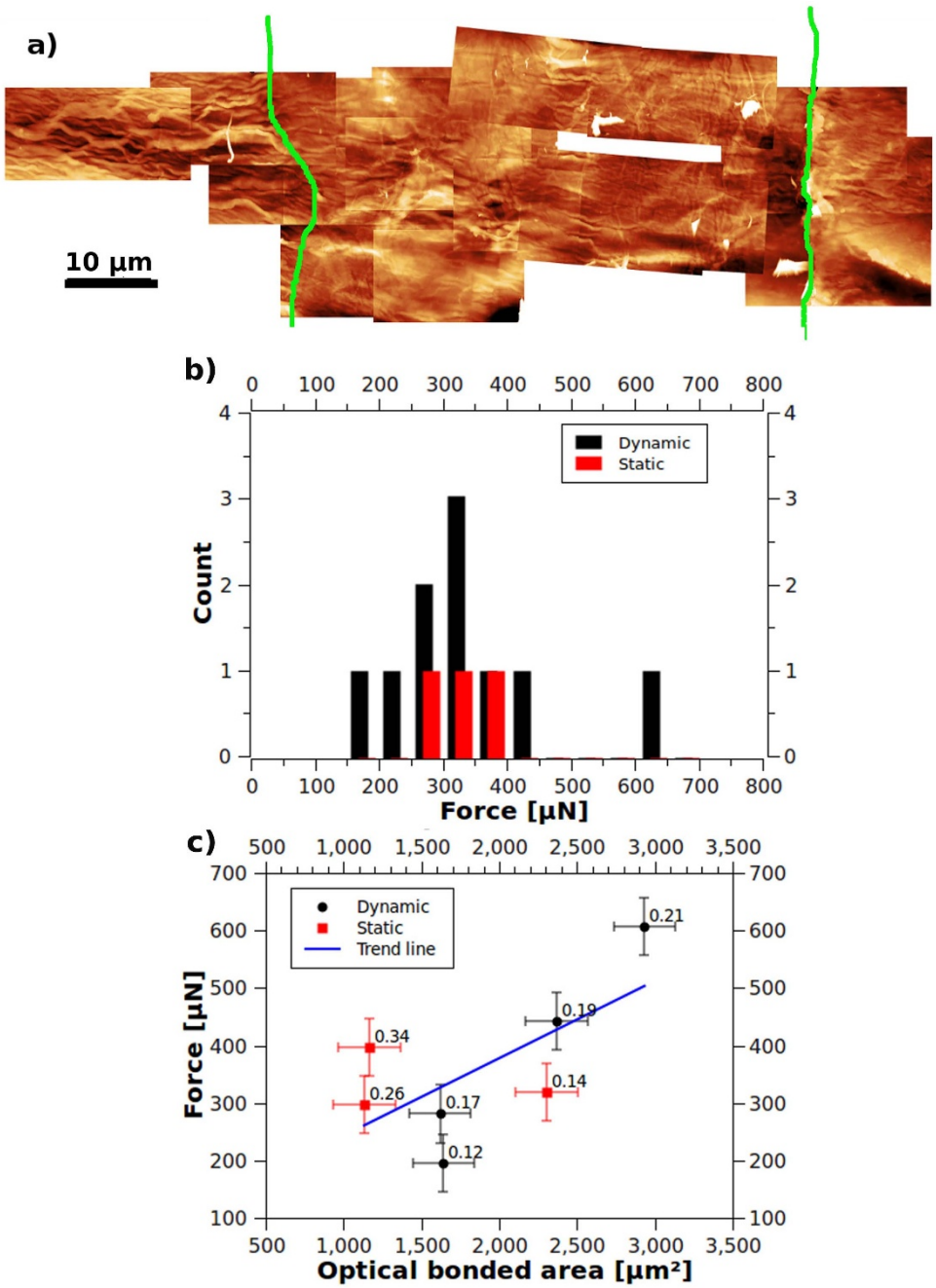

Figure 2 | **Summary of unrefined pulp investigations.** (a) AFM topography image reconstruction of the formerly bonded area. The green lines highlight the bonded area. Z-scale: 800 nm. (b) Histogram of the fracture test results and (c) plot of the force versus optical bonded area. The values next to the data points correspond to the specific bond strength [MPa].

Fracture tests analysis of unrefined pulp resulted in 332 ± 120 μN in dynamic mode when the failure occurred in the first loading cycle and 338 ± 52 μN for static loading of the fibre-fibre bonds (see Figure 2b). To explain the spread of data, we have to consider the large variation in fibre-fibre bonded area. Kappel et al.[44] measured bonded areas by microtomy and optical microscopy that range from 500 to 3000 μm^2. Comparison of the optically determined bonded area with the AFM image reconstruction demonstrated a 10% larger bonded area for the optical determination. Given the significant morphological differences between bonded and unbonded regions, an effect on bonding strength is expected. Therefore, Figure 2c correlates the fracture test data to the estimated bonded area from optical microscopy images taken prior to the experiment. The values next to the experimental data in the plot correspond to the bond strength of the optically determined bonded area, i.e., the specific bond strength. The question arises why even these values considerably scatter from 0.12 to 0.34 [MPa]. Besides the dependence on the bonded area other mechanisms play a significant role in holding two fibres together. These factors are the diversity of the fibre itself, morphological features like pits, which are holes in the cell wall that vary the fibre conformability[15], and the difference in residual strain from the prestraining of the top fibre. Another important aspect is the difference between the bonded area and the area in molecular contact. It has not been clear how much of the formerly bonded area is in molecular contact. All these factors allow for an increase in bond strength with the bonded area.

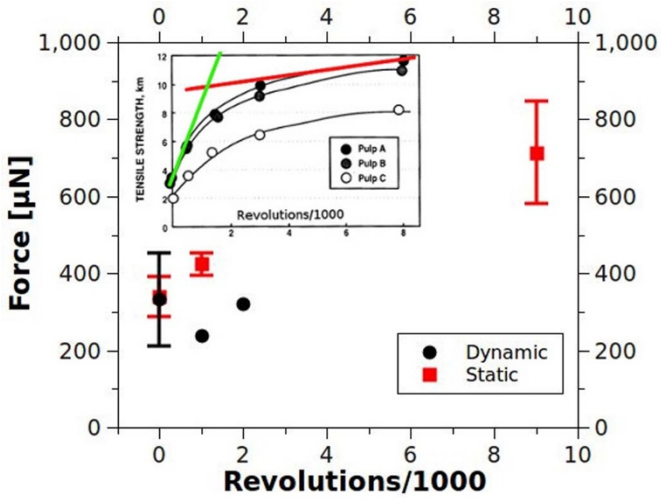

Figure 3 | Fracture test results of refined pulp. Joint strength force of single fibre-fibre bonds depending on refining tested in dynamic and static mode. The inset (after[46]) presents tensile index of sheets as a consequence of refining. A + B: northern species, C: southern species. The two solid lines indicate the change in slope of the curve.

An analysis of the various energy contributions provides deeper insight into bonding mechanics. For the unrefined pulp, 90% of the energy input was in the form of elastic energy. This large elastic fraction is attributed to deflection and twisting of the mounted top fibre. The total amount of viscoelastic energy is 1% of the energy input. With these energy contributions, a bond energy can be calculated. For the tested, unrefined pulp the energy input into the fibre-fibre bond is $10^{-13}-10^{-12}$ kJ/bond. Initial theoretical calculations predict bond energies between $10^{-16}-10^{-10}$ kJ/bond for the individual bonding mechanisms. These values, calculated from model bonds, are lower and upper bounds of bond energies. However, they are in good agreement with the experiment and literature data[45].

Not only the bonded area but also also modification of pulp itself influences the strength of paper[10]. Cowan presented data on how refining influences paper sheet strength[46], reporting that moderate beating up to 1000 revolutions strongly increased sheet strength (see inset of Figure 3). Beating with more revolutions (from 2000 to 9000 revolutions in a PFI mill[47]) resulted in only a slight increase of the tensile index. Figure 3 presents the data for single fibre-fibre bonds for refined pulp obtained from our method. Dynamic testing includes only data from first trials with refined pulps and shows no increase in paper strength with refining. However, static testing shows an increase in bond strength with beating.

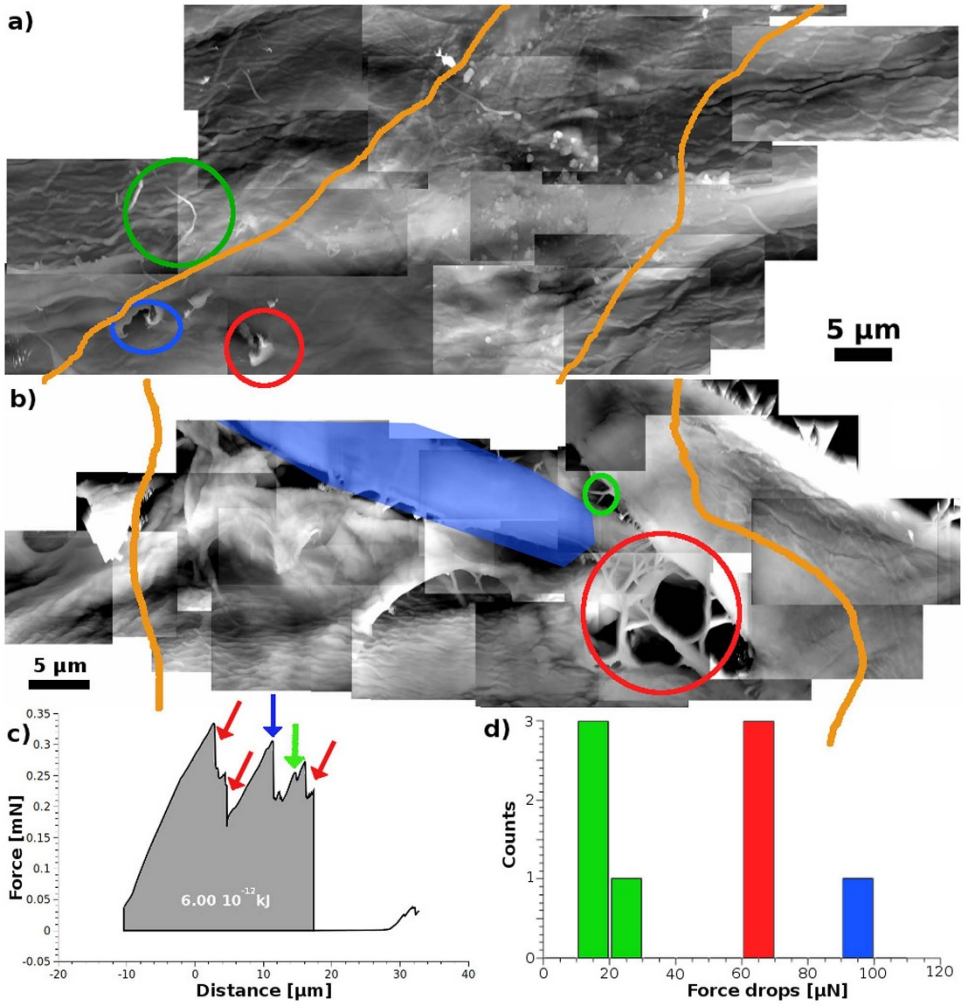

Figure 4 | Findings based on investigations of refined pulp. AFM topography image reconstruction of the formerly bonded area of (a) 1000 revolutions and (b) 2000 revolutions refined pulp. The orange lines highlight the bonded area. Green - single fibrils, Red - fibril bundles, and Blue - cell wall delamination. (c) Force versus distance curve of the bond in (b) representing force discontinuities and (d) classification of force drops presented in (c).

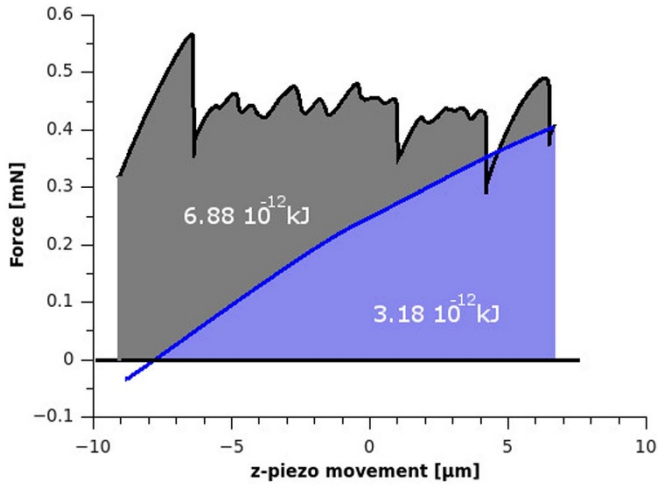

Figure 5 | Contribution of mechanical interlocks. Force-versus-distance of refined (9000 revolutions - PFI mill) and unrefined fiber-fiber bond. The additional gain of mechanical interlocks was calculated to be 55% of the bonds energy.

The influence of beating on the formerly bonded area is revealed in Figure 4. Figures 4a,b show AFM topography image reconstructions of the formerly bonded area for 1000 and 2000 revolutions in a PFI mill, respectively. In comparison to Figure 2a, Figure 4a reveals more of the longer single dangling fibrils (Ø = 40 nm, l = 10 μm, green circle). Furthermore, the onset of wall delamination is recognizable (marked by the blue circle). The more highly refined pulp (2000 revolutions - Figure 4b) differs completely from the unrefined pulp. Here, cell wall layer delamination is very pronounced, with several cellulose fibrils and fibril bundles acting as bridging elements between the delaminated walls (marked by the red circle). Figure 4c presents a force-versus-distance curve recorded during the breaking. This figure presents force discontinuities and provides support for the idea of bridging elements failing one after another. The recorded drops in force are classified in Figure 4d using a unique colour code. The classified breaking elements are: single fibrils (green), fibril bundles (red), and cell wall layers (blue). Experiments on pulp with 9000 revolutions resulted in stronger bonding strength but the dangling fibrils disturb the AFM feedback signal and made it impossible to inspect the formerly bonded area with the AFM.

In order to estimate the contribution of mechanical interlocks to the total energy input, a direct comparison of force-versus-distance curves from unrefined and refined pulp was performed in Figure 5. The black curve is taken from an experiment for refined pulp with 9000 revolutions PFI. The blue curve results from an experiment with unrefined pulp which was adjusted to the rupture point of the experiment from the refined pulp. The corresponding energy inputs were calculated as the area under the respective experimental curves. The contribution of the mechanical interlocking is the difference of the energy input from the refined pulp to the unrefined pulp. For the experiment of the refined pulp the energy input was $6.88 \cdot 10^{-12}$ kJ and $3.18 \cdot 10^{-12}$ kJ for the unrefined pulp. Please note that for the latter value the integration was only taken till the force crosses the x-axis. Without readjustment of the experiment from the refined pulp, the energy input for unrefined pulp would increase to $4.7 \cdot 10^{-12}$ kJ. Taking these two limits into account, the contribution for mechanical interlocking ranges from $3.2 \cdot 10^{-12}$ to $4.7 \cdot 10^{-12}$ kJ. Thus, it can be stated that for refined pulp with 9000 revolutions PFI the revealed mechanical interlocking mechanism increases the bond-strength by about 30–55%.

Taking into account all the information from the individual experiments, it is possible to explain the increase in sheet strength during refining. Initially, moderate beating increases the amount of dangling fibrils which can work as bridging elements to strengthen the fibre-fibre bond. After 2000 revolutions, however, the minimal further increase in paper sheet strength is almost negligible. This behaviour can be explained with an increase in fibre conformability and swelling[10] that results in more bonds and larger bonded area. In contrast to these enhancing effects, the formerly bonded area revealed cell wall delamination which is an indication for the natural limit of fibre-fibre bonds. Thus, only an increase in the number of fibre-fibre bonds leads to a stronger paper sheet.

Discussion

The controlled separation of two bonded paper fibres with a custom available AFM reveals breaking force and allows investigation of the force-versus-distance behaviour prior to failure. Static and dynamic loading grant access to elastic and viscoelastic mechanical properties and their contribution to the fibre-fibre bond (90% and 1%, respectively). Furthermore, imaging of the formerly bonded area uncovers the true three-dimensional surface area of the bonded region and revealed a smoother surface than the rest of the fiber. Here, dangling fibrils close to the transition zone between bonded and unbonded area are revealed. This fact clearly indicates that fibrils and fibril bundles act as mechanical interlocks or fibril bridges. This mechanical interlocking mechanism boosts the bond energy by a factor of 2 for the highly refined pulp (9000 revolutions PFI). In addition, the images of the formerly bonded area turned out to be an important basis for a new understanding of the formation of the bonds in the paper network. Here, the AFM data was recently used to calculate the effect of capillary bridges between the paper fibres. This overall ongoing investigation of fibre-fibre bonding helps to optimise an underestimated high-tech material which we use on a daily basis without giving much thought to its material properties. With this acquired knowledge on fibre bonding it will be possible to improve the strength of paper in a 400 Mt/a worldwide industry with simultaneous reductions in material, energy input, and environmental impact.

Methods

Fibre-fibre bonds were prepared from a dilute suspension of corresponding pulp with a consistency of 0.01% and put on PTFE foils for drying in a conventional sheet dryer[48]. After drying, individual fibre-fibre bonds were mounted across a gap on a specifically designed sample holder[37] with nail polish. The calibrated[49] cantilever ($k \sim 600 \frac{N}{m}$) of the AFM (Asylum Research MFP3D) applied load on the lower fibre, which was only connected to the top fibre in the fibre-fibre bond (see Figure 1). Depending on the loading - dynamic or static - it is feasible to study elastic or viscoelastic interaction[37]. Energy contributions were calculated from force-versus-distance curves. To determine exact travelling distance, a closed loop scanner[50] had to be employed, which was in our case an inductive sensor. Additionally, sequences of topography images of the bonded area were stitched together (see Figure 2a) and compared with the optically determined bonded area. All the experiments were conducted under ambient conditions ($20 \pm 2\ C^{\circ}$, $40 \pm 10\%\ RH$).

1. Rolland, J. P. & Mourey, D. A. (Eds.) Paper based Technology. *MRS Bulletin* **38**, 299–333 (2013).
2. Tobjoerk, D. & Oesterbacka, R. Paper Electronics. *Adv. Mater.* **23**, 1935–1961 (2011).
3. Zheng, G. *et al.* Nanostructured paper for flexible energy and electronic devices. *MRS Bulletin* **38**, 320–325 (2013).
4. Martinez, R. V., Fish, C. R., Chen, X. & Whitesides, G. M. Elastomeric Origami: Programmable Paper-Elastomer Composites as Pneumatic Actuators. *Adv. Funct. Mater.* **22**, 1376–1384 (2012).
5. Mirica, K. A., Weis, J. G., Schnorr, J. M., Esser, B. & Swager, T. M. Mechanical Drawing of Gas Sensors on Paper. *Angew. Chem.* **51**, 10740–10745 (2012).
6. Yang, G., Lee, C, Kim, J., Ren, F. & Pearton, S. J. Flexible graphene-based chemical sensors on paper substrates. *Phys. Chem. Chem. Phys* **15**, 1798–1801 (2013).
7. Fragouli, D. *et al.* Superparamagnetic cellulose fiber networks via nanocomposite functionalization. *J. Mater. Chem.* **22**, 1662–1666 (2012).
8. Bayer, I. S. Water-Repellent Cellulose Fiber Networks with Multifunctional Properties. *ACS Appl. Mater. Interfaces* **3**, 4024–4031 (2011).
9. Ayadi, F. *et al.* Mechanical reinforcement and water repellency induced to cellulose sheets by a polymer treatment. *Cellulose* **20**, 1501–1509 (2013).

10. Vainio, A. & Paulapuro, H. Interfiber bonding and fiber segment activation in paper. *BioResources* **2**, 442–458 (2007).
11. Rowell, R. *Handbook of wood chemistry and wood composites* (CRC Press, Boca Raton, 2005).
12. Lindström, T., Wågberg, L. & Larsson, T. On the nature of joint strength in paper–A review of dry and wet strength resins used in paper manufacturing. *Proc. 13th Fundamental Research Symp* (2005).
13. Haslach, H. Time-dependent mechanisms in fracture of paper. *Mech. Time-Depend. Mat.* **13**, 11–35 (2009).
14. Persson, B. Capillary adhesion between elastic solids with randomly rough surfaces. *J. Phys.-Condens. Mat.* **20**, 315007 (2008).
15. Stratton, R. A. & Colson, N. L. Dependence of fiber/fiber bonding on some papermaking variables. *IPST Technical Paper Series* **357**, 1–16 (1990).
16. Schniewind, A., Nemeth, L. & Brink, D. fibre and pulp properties I. Shear strength of single-fibre crossings. *Tappi* **47**, 244–248 (1964).
17. Mayhood Jr, C., Kallmes, O. & Cauley, M. The mechanical properties of paper. Part II: Measured shear strength of individual fibre to fibre contacts. *Tappi* **45**, 69–73 (1962).
18. Forstrom, J., Torgnysdotter, A. & Wågberg, L. Influence of fibre/fibre joint strength and fibre flexibility on the strength of papers from unbleached kraft fibres. *Nord. Pulp Pap. Res. J.* **20**, 186–191 (2005).
19. Torgnysdotter, A. & Wågberg, L. Tailoring of fibre/fibre joints in order to avoid the negative impacts of drying on paper properties. *Nord. Pulp Pap. Res. J.* **21**, 411–418 (2006).
20. Yu, Y., Tian, G., Wang, H., Fei, B. & Wang, G. Mechanical characterization of single bamboo fibres with nanoindentation and microtensile technique. *Holzforschung* **65**, 113–119 (2010).
21. Burgert, I., Frühmann, K., Keckes, J., Fratzl, P. & Stanzl-Tschegg, S. Microtensile testing of wood fibres combined with video extensometry for efficient strain detection. *Holzforschung* **57**, 661–664 (2003).
22. Lee, S., Wang, S., Pharr, G., Kant, M. & Penumadu, D. Mechanical properties and creep behavior of lyocell fibres by nanoindentation and nano-tensile testing. *Holzforschung* **61**, 254–260 (2007).
23. Salvetat, J. *et al.* Mechanical properties of carbon nanotubes. *Appl. Phys. A-Mater.* **69**, 255–260 (1999).
24. Demczyk, B. *et al.* Direct mechanical measurement of the tensile strength and elastic modulus of multiwalled carbon nanotubes. *Mat. Sci. Eng. A-Struct.* **334**, 173–178 (2002).
25. Yu, M., Files, B., Arepalli, S. & Ruoff, R. Tensile loading of ropes of single wall carbon nanotubes and their mechanical properties. *Phys. Rev. Lett.* **84**, 5552–5555 (2000).
26. Wang, Z. L. & Song, J. H. Piezoelectric nanogenerators based on zinc oxide nanowire arrays. *Science* **312**, 242–246 (2006).
27. van der Rijt, J. *et al.* Micromechanical testing of individual collagen fibrils. *Macromol. Biosci.* **6**, 697–702 (2006).
28. Cheng, Q. & Wang, S. A method for testing the elastic modulus of single cellulose fibrils via atomic force microscopy. *Compos. Part. A-Appl. S.* **39**, 1838–1843 (2008).
29. Shen, Z., Dodge, M., Kahn, H., Ballarini, R. & Eppell, S. Stress-strain experiments on individual collagen fibrils. *Biophys. J.* **95**, 3956–3963 (2008).
30. Naraghi, M., Ozkan, T., Chasiotis, I., Hazra, S. & de Boer, M. MEMS platform for on-chip nanomechanical experiments with strong and highly ductile nanofibres. *J. Micromech. Microeng.* **20**, 125022 (2010).
31. Gurnagul, N., Ju, S. & Page, D. S. Fibre-fibre bond strength of once-dried pulps. *J. Pulp Pap. Sci.* **27**, 88–91 (2001).
32. Suresh, S. *Fatigue of Materials* (Cambridge University Press, Cambridge, 1998).
33. Anderson, T. *Fracture mechanics: fundamentals and applications* (CRC Press, Boca Raton, 2005).
34. Haslach, H. The moisture and rate-dependent mechanical properties of paper: a review. *Mech. Time-Depend. Mat.* **4**, 169–210 (2000).
35. Habeger, C., Coffin, D. & Hojjatie, B. Influence of humidity cycling parameters on the moisture-accelerated creep of polymeric fibres. *J. Polym. Sci. Pol. Phys.* **39**, 2048–2062 (2001).
36. Binnig, G., Quate, C. & Gerber, C. Atomic Force Microscope. *Phys. Rev. Lett.* **56**, 930–933 (1986).
37. Schmied, F., Teichert, C., Kappel, L., Hirn, U. & Schennach, R. Joint strength measurements of individual fiber-fiber bonds - an atomic force microscopy based method. *Rev. Sci. Instrum.* **83**, 073902 (2012).
38. Ishikawa, K., Okuda, H. & Kobayashi, Y. Creep of pure aluminium materials at a low temperature. *J. Mater. Sci. Lett.* **17**, 423–424 (1998).
39. Nanko, H. & Ohsawa, J. Mechanisms of fibre bond formation. *Fundamentals of papermaking: transactions of the Ninth Fundamental Research Symposium held at Cambridge* **783** (1989).
40. Keckes, J. *et al.* Cell-wall recovery after irreversible deformation of wood. *Nature Materials* **2**, 810–813 (2003).
41. Fratzl, P., Burgert, I. & Keckes, J. Mechanical model for the deformation of the wood cell wall. *Zeitschrift für Metallkunde* **95**, 579–584 (2004).
42. Altaner, C. & Jarvis, M. Modelling polymer interactions of the 'molecular Velcro' type in wood under mechanical stress. *Journal of Theoretical Biology* **253**, 434–445 (2008).
43. Persson, B. *et al.* Adhesion of cellulose fibers in paper. *J. Phys.: Condens. Matter* **25**, 045002 (2013).
44. Kappel, L., Hirn, U., Gilli, E., Bauer, W. & Schennach, R. Revisiting polarized light microscopy for fibre-fibre bond area measurement - Part II: Proving the applicability. *Nord. Pulp Pap. Res. J.* **25**, 71–75 (2010).
45. Stratton, R. A. Characterization of fibre-fibre bond strength from paper mechanical properties. *IPST Technical Paper Series* **381**, 1–32 (1991).
46. Cowan, W. Explaining handsheet tensile and tear in terms of fiber-quality numbers. *Tappi Press* **78**, 101–110 (1995).
47. Levlin, J., Söderjhelm, L. & Yhdistys, S. *Pulp and paper testing* (Fapet Oy Finland, 1999).
48. Kappel, L., Hirn, U., Gilli, E., Bauer, W. & Schennach, R. A novel method for the determination of bonded area of individual fibre-fibre bonds. *Nord. Pulp Pap. Res. J.* **24**, 199–205 (2010).
49. Sader, J., Chon, J. & Mulvaney, P. Calibration of rectangular atomic force microscope cantilevers. *Rev. Sci. Instrum.* **70**, 3967 (1999).
50. Schneir, J., McWaid, T., Alexander, J. & Wilfley, B. Design of an atomic force microscope with interferometric position control. *J. Vac. Sci. Technol. B* **12**, 3561–3566 (1994).

Acknowledgements

The financial support of Mondi, Frantschach, and the Federal Ministry of Economy, Family and Youth and the National Foundation for Research, Technology and Development, Austria, is gratefully acknowledged. We thank Leo Arpa, Walter Ruef, Eduard Gilli, Otmar Kolednik, and Max G. Lagally for valuable discussions as well as Katherine Tiede for language edition.

Author contributions

F.S. and C.T. performed the experiments and analysed the data; L.K., U.H. and W.B. prepared the fiber-fiber bonds; R.S. organized overall collaboration; F.S., C.T. and U.H. wrote the paper; All authors discussed the results and commented on the manuscript.

Additional information

Competing financial interests: The authors declare no competing financial interests.

How to cite this article: Schmied, F.J. *et al.* What holds paper together: Nanometre scale exploration of bonding between paper fibres. *Sci. Rep.* **3**, 2432; DOI:10.1038/srep02432 (2013).